



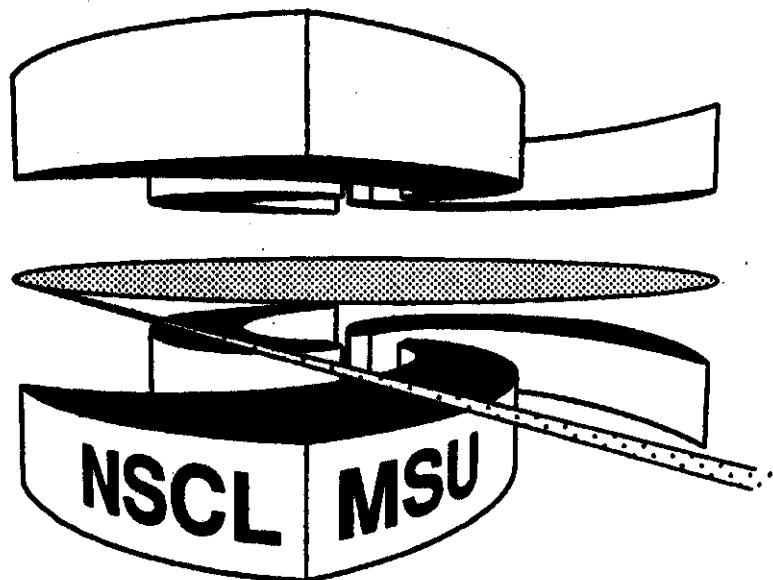
Michigan State University

National Superconducting Cyclotron Laboratory

**STUDY OF THE GIANT DIPOLE RESONANCE BUILT ON
HIGHLY-EXCITED STATES VIA
INELASTIC ALPHA-SCATTERING**

**Invited Talk Presented at the IV International Conference On Selected
Topics In Nuclear Structure, 5-9 July 1994, Dubna, Russia**

**M. THOENNESSEN, E. RAMAKRISHNAN, T. BAUMANN,
A. AZHARI, R.A. KRYGER, R. PFAFF, S. YOKOYAMA,
J.R. BEENE, F.E. BERTRAND, M.L. HALBERT, G. VAN BUREN,
R.J. CHARITY, J.F. DEMPSEY, P-F. HUA, D.G. SARANTITIES,
and L.G. SOBOTKA**



Study of the Giant Dipole Resonance Built on Highly-Excited States via Inelastic Alpha-Scattering

M. Thoennessen, E. Ramakrishnan, T. Baumann, A. Azhari,
R. A. Kryger, R. Pfaff, and S. Yokoyama

*National Superconducting Cyclotron Laboratory and
Department of Physics & Astronomy,
Michigan State University, East Lansing, Michigan 48824, USA*

J. R. Beene, F. E. Bertrand, M. L. Halbert,
P. E. Mueller, D. W. Stracener, and R. L. Varner

Oak Ridge National Laboratory, Oak Ridge, Tennessee 37831, USA

G. Van Buren, R. J. Charity, J. F. Dempsey, P-F. Hua,
D. G. Sarantites, and L. G. Sobotka

*Department of Chemistry, Washington University,
St. Louis, Missouri 63130, USA*

Abstract

High energy γ rays were measured in coincidence with inelastically scattered α particles at beam energies of 40 MeV/nucleon (on ^{120}Sn and ^{208}Pb targets) and 50 MeV/nucleon (on ^{120}Sn). High energy target excitations were observed and the giant dipole resonance (GDR) built on these excited states was measured by its γ -ray decay. The width of the GDR increases with excitation energy. This increase is not as strong as in the corresponding fusion-evaporation reactions.

1. INTRODUCTION

In recent years the study of the giant dipole resonance (GDR) built on highly excited states has yielded important information on the nuclear structure of hot nuclei [1, 2] and on reaction dynamical effects [3, 4]. Typically, the GDR is observed by its γ -ray decay following heavy-ion fusion reaction. The well established dependence of the parameters of the GDR strength function on nuclear size and deformation makes it possible to use the GDR to explore shape evolution as a function of excitation energy and angular momentum.

A systematic effort to explore the evolution of the GDR as a function of increasing excitation energy has recently been made, using heavy-ion fusion evaporation reactions. Two particularly interesting aspects are an increase in width of the GDR with increasing bombarding energy [5], and the apparent disappearance of GDR strength at very high energies [6]. The increase in excitation energy with increasing bombarding energy in a heavy-ion fusion reaction is accompanied by an increase in the mean angular momentum of the compound nucleus. Consequently it has not been possible to disentangle the effects of increasing angular momentum from those of the increase in excitation energy.

We used a different approach in order to separate the effects of angular momentum and excitation energy on the increase of the GDR width. Small-angle inelastic scattering

of light or heavy ions can populate highly excited states without transferring large amounts of angular momenta. It should therefore be possible to study the GDR as a function of excitation energy independent of angular momentum. However, two main conditions have to be fulfilled: (i) The cross section for large energy losses of the inelastically scattered particles must be dominated by target excitation and should not be due to other processes, for example projectile pickup and sequential decay or nucleon or cluster knock-out; and (ii) If the inelastic particle spectrum is predominantly due to target excitation, these excited states have to equilibrate rapidly, so that the subsequent decay can be described within the statistical model. The GDR built on highly excited states should then be observed in the same way as in fusion-evaporation reactions.

2. EXPERIMENTS AND DATA ANALYSIS

The experiments were performed at the National Superconducting Cyclotron Laboratory at Michigan State University (MSU). Isotopically enriched 3 mg/cm^2 ^{208}Pb and 16.8 mg/cm^2 ^{120}Sn targets were bombarded with 40 MeV/A α particles. The experiment on the ^{120}Sn target was also performed at 50 MeV/A . The inelastically scattered α particles were detected in the Washington University Dwarf Wall [7] which consisted of 35 CsI(Tl) detectors, covering angles between 12° and 36° . The discrimination of the inelastically scattered α particles from other light charged particles (p,d,t, ^3He) was achieved by pulse shape analysis. High energy γ rays were measured with the Oak Ridge National Laboratory BaF₂ array consisting of 76 detectors arranged in four arrays of 19 crystals each and a fifth array from MSU. The arrays were centered at 60° , 90° and 120° and covered total solid angle of $\sim 10\%$ of 4π . The γ -ray energy deposited in seven neighboring detectors was summed to improve the response of the detectors. Separation between γ rays and neutrons was achieved by time-of-flight. In addition, light charged particles at larger angles not covered by the Dwarf Wall were detected with the Dwarf Ball [7].

2.1. Alpha Spectra

It is essential to show that the spectra of the scattered α particles are dominated by target excitations and to understand the contributing background processes before any detailed analysis of the γ -ray spectra can be performed.

The top row of Figure 1 shows the inelastic α spectra integrated over all measured angles at $E_\alpha = 200 \text{ MeV}$ on ^{120}Sn (left) and $E_\alpha = 160 \text{ MeV}$ on ^{208}Pb (right). It shows the relatively slow decrease of the cross section towards lower α energies, corresponding to higher target excitation energies. The bottom row of Figure 1 shows the same spectra in coincidence with γ rays ($E_\gamma > 4 \text{ MeV}$). The clearly observed peak structure is due to the successive opening of neutron evaporation thresholds. These structures have been previously observed [8, 9] and are strong evidence for an equilibrated system up to at least $\sim 50 \text{ MeV}$. This observation is also consistent with the analysis of neutron spectra following inelastic α scattering [10].

In Figure 2 the α spectrum is extended to even lower α (higher excitation) energies for the two beam energies on the ^{120}Sn target. It shows a rapid increase of the cross section at apparent high target excitation energies. Previous measurements of inelastic α scattering at comparable incident energies did not include these high excitation energies [11, 12, 13]. The rise at these energies is too large to result from evaporated α particles following fusion. These α particles correspond to pre-equilibrium emission where the observed α is not necessarily the initially scattered α particle, but could be an α from the target. This is also supported by the comparison of the two beam energies shown in Figure 2. The shapes of the spectra scale with the α energy and not with the α energy loss. These processes have been studied in similar reactions [14, 15, 16] and can

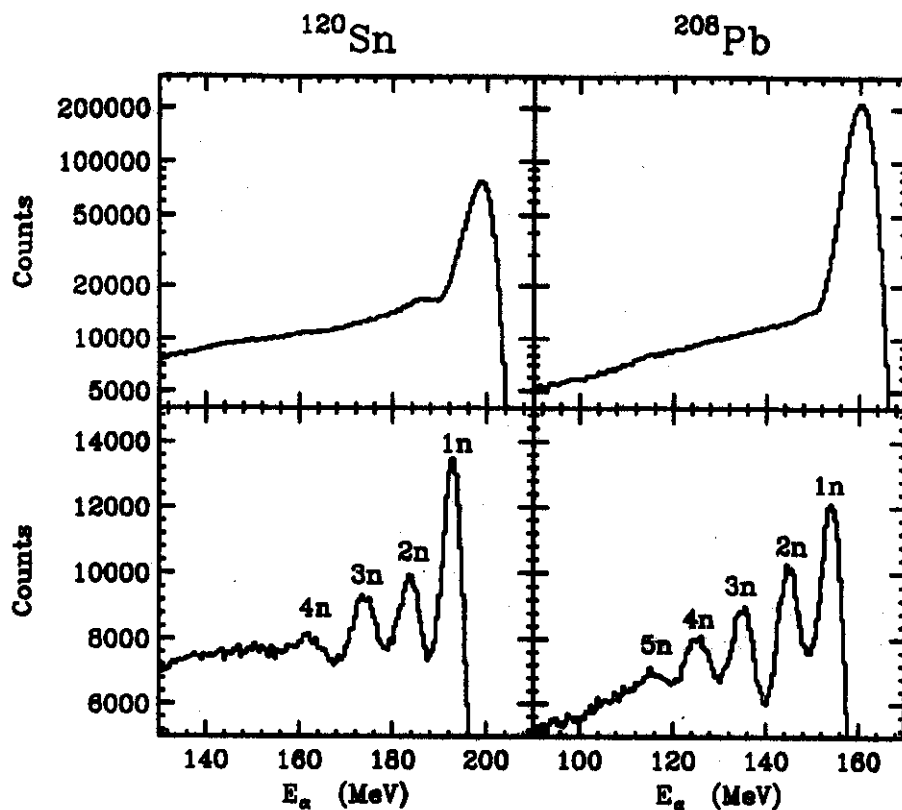


Figure 1: Inelastic α singles spectra (top) and in coincidence with γ rays (bottom) at $E_\alpha = 200$ MeV on ^{120}Sn (left) and at $E_\alpha = 160$ MeV on ^{208}Pb (right). The peaks in the coincidence data correspond to the successive opening of neutron evaporation channels as described in the text.

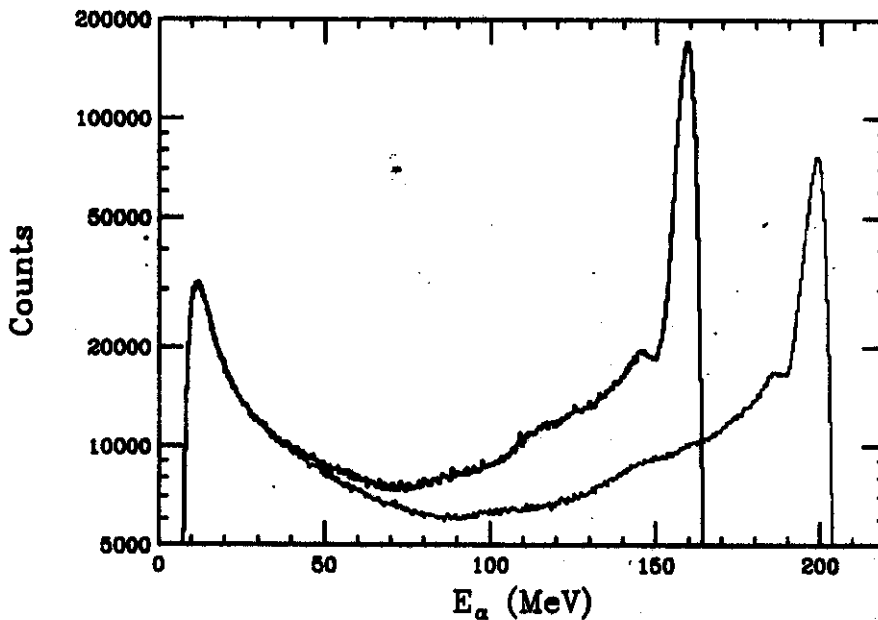


Figure 2: Inelastic α singles spectra at $E_\alpha = 200$ MeV and $E_\alpha = 160$ MeV on ^{120}Sn .

be explained within the multistep direct emission model [17, 18]. Detailed calculations of this type for the present data are under way [19].

Other processes that contribute to the α energy spectra are neutron [20] and proton [21] pickup by the projectile and subsequent decay. Due to the large solid angle coverage of the Dwarf-Ball/Wall for charged particles it is possible to extract the proton pickup-decay contribution and estimate the neutron pickup-decay contribution to the total spectrum. The contribution of these processes to the high energy γ -ray spectra is negligible, since they result in relatively low residual target excitation energies.

2.2 Gamma-Ray Spectra

Another confirmation of high target excitation energy is provided by the γ -ray spectra presented in Figure 3. The γ -ray spectra shown in the left panel were obtained by gating on the same α energy for the two incident beam energies on the ^{120}Sn target. The two spectra are clearly different with a more prominent contribution in the region of the GDR at the higher bombarding energy indicating a higher excitation energy. However, when the γ -ray spectra are gated on the same apparent excitation energy of 40-50 MeV, corresponding to α energies of 110-120 MeV and 150-160 MeV for the incident energies of 160 MeV and 200 MeV respectively (Figure 3, right), they are essentially identical within the statistical uncertainties.

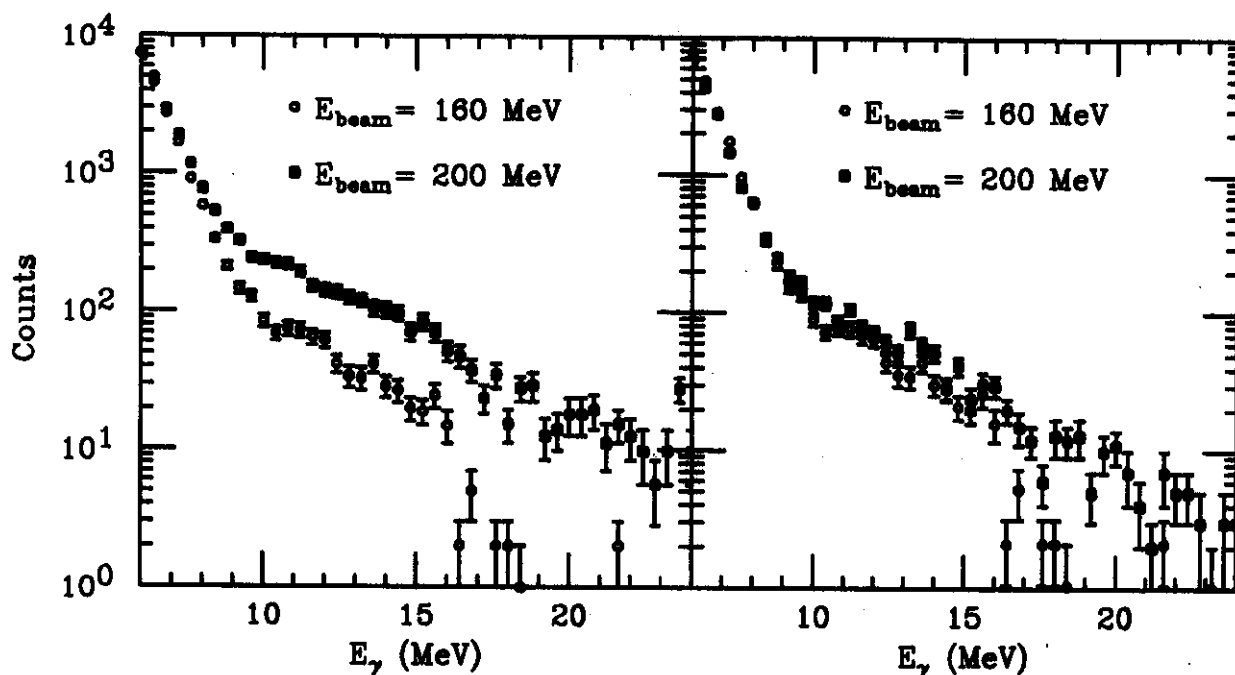


Figure 3: Comparison of the γ -ray spectra at $E_{\text{beam}} = 200$ MeV (■) and $E_{\text{beam}} = 160$ MeV (○) on ^{120}Sn gated on the same scattered α energy range (110-120 MeV, left) and the same α energy-loss (target excitation energy) range (40-50 MeV, right).

Figure 4 presents further evidence that the γ -ray spectra reflect the GDR built on highly excited states of the target nucleus. The spectra for the ^{208}Pb and the ^{120}Sn targets at excitation energies of 120-130 MeV were divided by the identical statistical model (CASCADE) calculation which did not include a GDR strength function. With this method the spectra can be compared on a linear scale. It is evident that the ^{208}Pb spectrum exhibits a peak at lower energies compared to the ^{120}Sn spectra. This is consistent with the measured mean ground state GDR energies which are 13.5 MeV and 15.4 MeV for ^{208}Pb and ^{120}Sn , respectively [22].

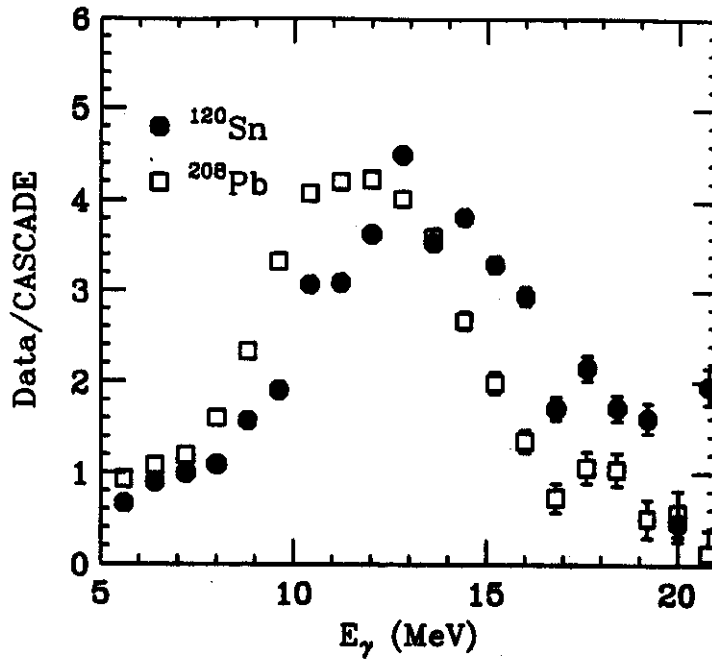


Figure 4: Experimental γ -ray spectra for the ^{208}Pb (\square) and the ^{120}Sn (\bullet) targets divided by a statistical model (CASCADE) calculation assuming a constant γ -ray strength function.

3. RESULTS

The γ -ray spectra in coincidence with the inelastically scattered α particles exhibited no statistically significant differences for either different angles of the γ -ray detectors or for different α scattering angles. Thus the γ -ray spectra of all five arrays were summed together. γ -ray spectra for 10 MeV wide excitation energy bins were created. Statistical model calculations using CASCADE [23] were performed and the calculated γ -ray spectra were folded with the response function for the detectors before they were compared with the data. The excitation energy spread in the α spectra for each bin of 10 MeV was used as the initial population distribution for CASCADE. This distribution was spread over an assumed angular momentum transfer of $0-5\hbar$.

Figure 5 shows fits for the energy bins of 60-70 MeV (left) and 90-100 MeV (right) for the ^{120}Sn target. The extracted width increases from $\Gamma_{GDR} = 7.7$ MeV to $\Gamma_{GDR} = 8.7$ MeV over this excitation energy range. The resonance energy for these preliminary calculations was kept constant at the ground state value of $E_{GDR} = 15.4$ MeV.

The preliminary results for the extracted widths are shown in Figure 6. The left side of the figure compares the present results from the inelastic scattering data on ^{120}Sn with fusion-evaporation data on ^{110}Sn [24]. The excitation energies plotted for the fusion data were corrected for the average rotational energy, determined from the calculated mean angular momentum populated in the reactions. The dashed line corresponds to an almost quadratic increase of the width with excitation energy as was shown in Ref. [24]. However, the width increase in the present inelastic scattering data is approximately linear as indicated by the solid line. This difference indicates that the width increase is partially due to the increase in excitation energy and partially due to the increase of angular momentum. Detailed free energy surface calculations need to be performed so that an analysis similar to Ref. [25] can be carried out in order to quantify our conclusions.

In order to compare the width of the ^{120}Sn with the ^{208}Pb data, the extracted widths are plotted as a function of temperature, calculated as $T = \sqrt{E^*/a}$ with the level density parameter $a = A/9$. The width increase in ^{208}Pb is also linear with increasing excitation

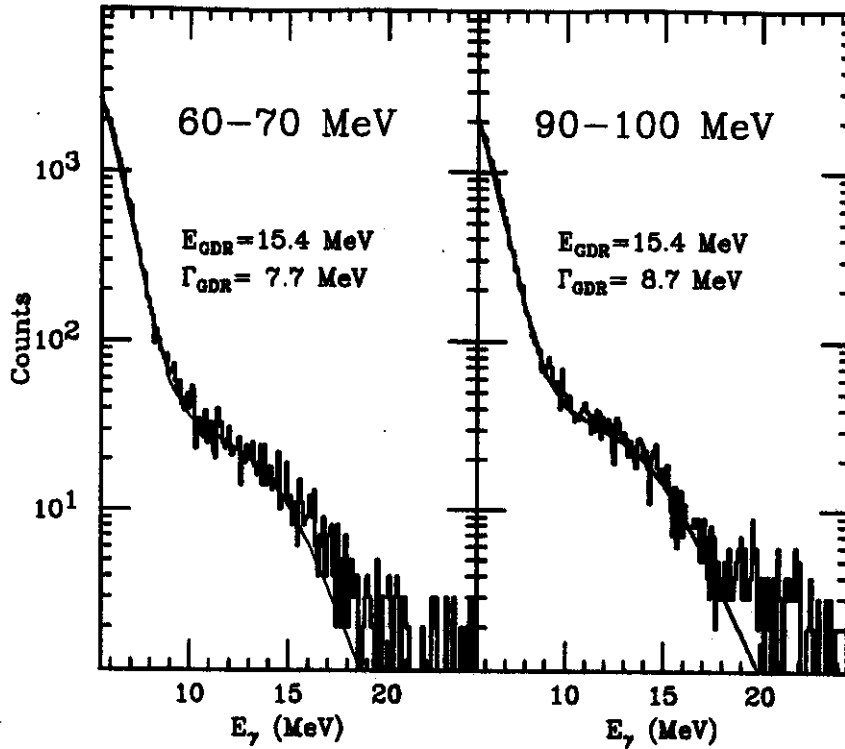


Figure 5: Sample γ -ray spectra and results of CASCADE calculations (smooth curve) for the ^{120}Sn target at excitation energies of 60-70 MeV (left) and 90-100 MeV (right).

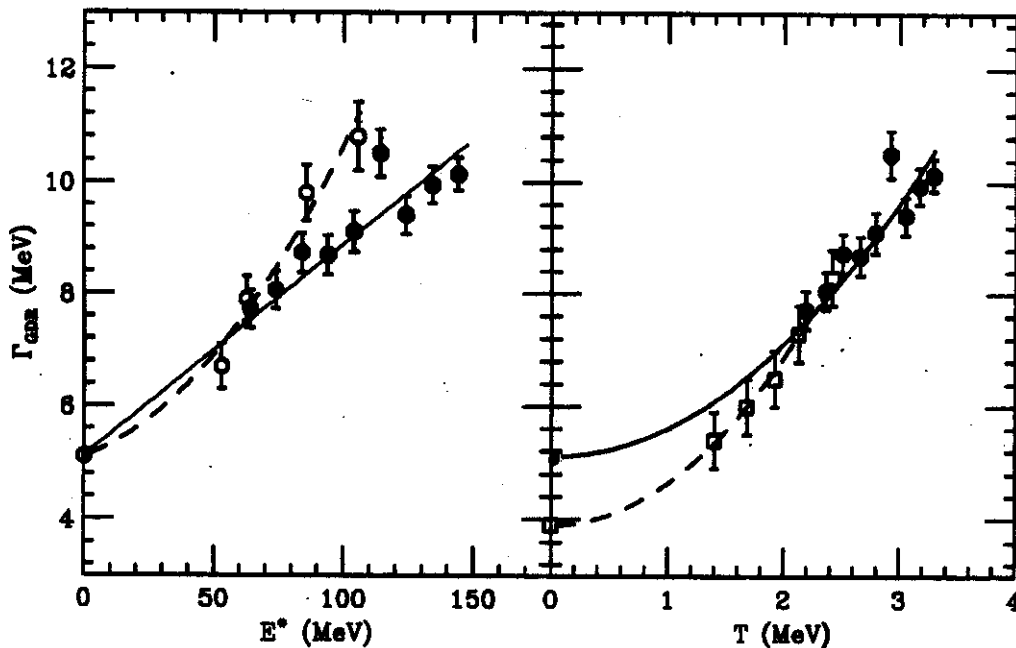


Figure 6: The width of the GDR as a function of excitation energy in ^{120}Sn (left) for fusion-evaporation measurements (from Ref. [24], \circ) and inelastic scattering (\bullet) and as a function of temperature (right) in ^{120}Sn (\bullet) and ^{208}Pb (\square).

energy, and therefore quadratic with temperature as shown by the dashed line in Figure 6. Although the analysis is still preliminary, the figure indicates a stronger increase in ^{208}Pb compared to ^{120}Sn . This observation is consistent with potential energy calculations [26] for both systems as a function of temperature. The free energy surface calculations for ^{208}Pb show a steeper surface at low temperatures due to the doubly closed shell. However the shell structure effects wash out rather rapidly between 1 and 2 MeV. This results in a rather rapid broadening of the minimum of the free energy surface and thus could explain the larger increase of the GDR width.

4. SUMMARY AND CONCLUSIONS

Inelastic α scattering was used to populate highly excited states of the target nucleus. These states equilibrate quickly so that their decay can be treated within the statistical model. Thus it is possible to study the GDR built on these excited states by their γ -ray decay. The advantage of inelastic scattering reactions over fusion-evaporation reactions is that relatively low angular momentum states are populated, almost independent of the excitation energy. The excitation energy dependence of the GDR width can therefore be studied with little influence from increasing angular momentum. In the first application of this method we studied ^{208}Pb and ^{120}Sn . The preliminary analysis shows that in ^{120}Sn the width increase with increasing excitation energy is smaller than in fusion reactions, indicating that the increase observed in fusion reactions is only partly due to excitation energy, with a significant contribution from angular momentum increase. The comparison between the ^{120}Sn and the ^{208}Pb data seems to show a stronger increase for ^{208}Pb . This observation is in qualitative agreement with free energy surface calculations, and can be interpreted in terms of the vanishing of shell effects.

5. ACKNOWLEDGMENTS

This work was partially supported by the U.S. National Science Foundation under grant No. PHY-92-14992 and by the Department of Energy under grants No. DE-FG01-88ER40406 and DE-FG02-87ER40310. Oak Ridge National Laboratory is managed by Martin Marietta Energy Systems, Inc. under contract DE-AC05-84OR21400 with the Department of Energy.

6. REFERENCES

- [1] K. A. Snover, *Ann. Rev. Nucl. Part. Sci.* 36, 545 (1986).
- [2] J. J. Gaardhøje, *Ann. Rev. Nucl. Part. Sci.* 42, 483 (1992).
- [3] M. Thoennessen, J. R. Beene, F. E. Bertrand, C. Baktash, M. L. Halbert, D. J. Horen, D. G. Sarantites, W. Spang, and D. W. Stracener, *Phys. Rev. Lett.* 70, 4055 (1993).
- [4] P. Paul and M. Thoennessen, *Ann. Rev. Nucl. Part. Sci.* 44, in press (1994).
- [5] A. Bracco, *et al.*, *Phys. Rev. Lett.* 62, 2080 (1989).
- [6] J. Kasagi and K. Yoshida, *Nucl. Phys. A* 569, 195c (1994), T. Suomijärvi, *et al.* *Nucl. Phys. A* 569, 225c (1994), and references therein.
- [7] D. W. Stracener, D. G. Sarantites, L. G. Sobotka, J. Elson, J. T. Hood, Z. Majka, V. Abenante, A. Chbihi, and D. C. Hensley, *Nucl. Instr. and Meth. A* 294, 485 (1990).
- [8] M. T. Collins, C. C. Chang, S. L. Talbor, G. J. Wagner, and J. R. Wu, *Phys. Rev. Lett.* 42, 1440 (1979), M. T. Collins, C. C. Chang, and S. L. Talbor, *Phys. Rev. C* 24, 387 (1981).

- [9] M. Thoennessen, *et al.*, Phys. Rev. C 43, R12 (1991).
- [10] A. van der Woude, Nucl. Phys. A 482, 453c (1988).
- [11] H. W. Ho and E. M. Henley, Nucl. Phys. A 225, 205 (1974).
- [12] D. H. Youngblood, J. M. Moss, C. M. Rozsa, J. D. Bronson, A. D. Bacher, and D. R. Brown, Phys. Rev. C 13, 994 (1976), J. M. Moss, D. R. Brown, D. H. Youngblood, C. M. Rozsa, and J. D. Bronson, Phys. Rev. C 18, 741 (1978).
- [13] F. E. Bertrand, G. R. Satchler, D. J. Horen, J. R. Wu, A. D. Bacher, G. T. Emery, W. P. Jones, D. W. Miller, and A. van der Woude, Phys. Rev. C 22, 1832 (1980).
- [14] T. Chen, R. E. Segel, P. T. Debevec, J. Wiggins, P. P. Singh, and J. V. Maher, Phys. Lett. B 103, 192 (1981).
- [15] G. Ciangaru, C. C. Chang, H. D. Holmgren A. Nadasen, P. G. Roos, A. A. Cowley, S. Mills, P. P. Singh, M. K. Saber, and J. R. Hall, Phys. Rev. C 27, 1360 (1983), G. Ciangaru, C. C. Chang, H. D. Holmgren A. Nadasen, and P. G. Roos, Phys. Rev. C 29, 1289 (1984).
- [16] W. A. Richter, A. A. Cowley, R. Lindsay, J. J. Lawrie, S. V. Förtsch, J. V. Pilcher, R. Bonetti, and P. E. Hodgson, Phys. Rev. C 46, 1030 (1992).
- [17] H. Feshbach, A. Kerman, and S. Koonin, Ann. Phys. 125, 129 (1980).
- [18] R. Bonetti, M. B. Chadwick, P. E. Hodgson, B. V. Carlson, and M. S. Hussein, Phys. Rep. 202, 173 (1991),
- [19] M. Hussein and M. Chadwick, private communication.
- [20] D. R. Brown, I. Halpern, J. R. Calarco, P. A. Russo, D. L. Hendrie, and H. Homeyer, Phys. Rev. C 14, 896 (1976).
- [21] A. Saha, R. Kamermans, J. van Driel, and H. P. Morsch, Phys. Lett. B 79, 363 (1978).
- [22] S. Dietrich and B. Berman, At. Data Nucl. Data Tables, 38, 208 (1988).
- [23] F. Pühlhofer, Nucl. Phys. A 260, 276 (1977).
- [24] D. R. Chakrabarty, S. Sen, M. Thoennessen, N. Alamanos, P. Paul, R. Schicker, J. Stachel, and J. J. Gaardhøje, Phys. Rev. C 36, 1886 (1987).
- [25] Y. Alhassid and B. Bush, Phys. Rev. Lett. 65, 2527 (1990).
- [26] T. Werner, private communication.